Evaluation The Effectiveness of Some Consolidants for Preservation of Limestone in Hathor Temple at Memhis, Egypt

Dr. Ahmed Ibrahim Manci

Conservation Dept., Faculty of Archaeology and Tourism Guidance, Misr University for Science & Technology, Egypt

ahmed.ibrahim@must.edu.eg

Abstract

Memphis city is the first capital of ancient Egypt; it's considered to be an open-air museum for the ancient Egyptian archaeological buildings. Twenty kilometers south of Giza, the modern village of Mit- Rahina lies at the core of Memphis city. Hathor temple is one of the most important archaeological building in Mit- Rahina village, it was built of limestone by Ramesses II (the 19th Dynasty). The temple is being comprised of a partially exposed colonnaded hall on the north, and that hall has spectacular capitals in the traditional form of Hathor as a human visage with bovine ears. The temple was affected by several deterioration phenomena and patterns of damage which occurred as time went by, as a result of being exposed to many aggressive factors. The assessment of the current conservation state of the temple were performed, including studying the properties of limestone which is the main construction material of Hathor temple using X-ray diffraction, polarizing light microscopy (PLM) and the scanning electron microscopy (SEM). The experimental study was performed on samples of limestone using four consolidants to choose the best consolidant to the conservation of Hathor temple. To evaluate the consolidants, the physical and the mechanical properties of the treated samples were estimated, also aesthetical properties by visual examination, colorimetric measurements, as well as static water contact angle and the morphologic study using the scanning electron microscopy (SEM). The evaluation methodology of consolidants efficiency is performed by comparing properties of the treated samples together, then comparing them with properties of untreated samples. Stability and efficiency of the consolidants were evaluated by repeating the measurement of static water contact angle for the treated samples after exposure to the artificial aging cycles. The study indicated that the most important deterioration factor affecting the temple is a salty ground water. The results obtained from studying the archeological limestone by investigation and analytical methods which showed that it is consisting mainly of very fine grains of calcite, with minor amount of dolomite and rare quartz, opaque minerals, iron oxides and halite, with microfossils. It also suffers from different kinds of degradation phenomena. The experimental study results showed that the nanocomposite (Nanorestor + M.T.M.O.S) is the most suitable for consolidation and protection of the limestone samples, as it showed higher compatibility in physio-chemical, mechanical and aesthetical properties with the limestone material and the best for resistance to artificial aging procedures, compared by other consolidants in this study.

Key Worde

Limestone, consolidation, mechanical properties, physical properties, water contact angle.

الملخص

مدينة ممفيس هي أول عاصمة لمصر القديمة. تعتبر متحف مفتوح للمباني الأثرية المصرية القديمة. تقع قرية ميت رهينة الحالية على بعد عشرين كيلومترًا إلى الجنوب من الجيزة في قلب مدينة ممفيس. يعتبر معبد حتحور من أهم المباني الأثرية في قرية ميت رهينة، وقد شيده رمسيس الثاني (الأسرة التاسعة عشر) من الحجر الجيري. يتكون المعبد من قاعة اعمدة مكشوفة جزئياً في الشمال، هذه القاعة لها تيجان رائعة على الشكل التقليدي لحتحور كمظهر بشري بآذان بقرية. تأثر المعبد بالعديد من مظاهر التلف وأنماط الضرر بمرور الوقت، نتيجة تعرضه للعديد من عوامل التلف العدوانية. تم إجراء تقييم لحالة الحفظ الحالية للمعبد، بما في ذلك دراسة خصائص الحجر الجيري الذي يعد مادة البناء الرئيسية باستخدام حيود الأشعة السينية، والفحص بالميكروسكوب المستقطب (PLM) والفحص بالميكروسكوب الإلكتروني الماسح (SEM). تم إجراء الدراسة التجريبية على عينات من الحجر الجيري باستخدام أربعة مواد تقوية لاختيار أفضلهم في معالجة وصيانة معبد حتحور. لتقييم مواد التقوية، تم تقدير الخواص الفيزيائية والميكانيكية للعينات المعالجة، كما تم تقدير الخصائص الجمالية عن طريق الفحص البصري، وقياس التغيرات اللونية، وكذلك قياس زاوية تلامس الماء الساكن مع سطح العينات المعالجة والدراسة باستخدام الميكروسكوب الإلكتروني الماسح (SEM). يتم تنفيذ منهجية تقييم كفاءة مواد التقوية من خلال مقارنة خصائص العينات المعالجة معاً، ثم مقارنتها بخصائص العينات غير المعالجة. تم تقييم ثبات وكفاءة مواد التقوية من خلال تكرار قياس زاوية التلامس مع الماء الساكن للعينات المعالجة بعد التعرض لدورات التجوية الصناعية. أوضحت الدراسة أن أهم عامل تدهور يؤثر على المعبد هو المياه الجوفية المالحة. أظهرت النتائج التي تم الحصول عليها من دراسة الحجر الجيري الأثري بطرق الفحص والتحليل أنه يتكون أساسًا من حبيبات دقيقة جدًا من الكالسيت، مع كمية قليلة من الدولوميت والكوارتز النادر، والمعادن غير الشفافة، وأكاسيد الحديد والهاليت، مع أحافير دقيقة، كما أنه يعاني من أنواع مختلفة مظاهر التلف. أظهرت نتائج الدراسة التجريبية أن المركب النانوي (Nanorestor + M.T.M.O.S) هو الأنسب لتوحيد وحماية عينات الحجر الجيري. حيث أظهرت توافقًا أعلى في الخواص الفيزيائية والكيميائية والميكانيكية والجمالية مع مادة الحجر الجيري مقارنة بمواد التقوية الأخرى فى هذه الدراسة.

الكلمات المفتاحية

الحجر الجيري، التقوية، الخواص الميكانيكية، الخصائص الفيزيائية، زاوية ملامسة الماء.

1. INTRODUCTION

Hathor temple is situated in Mit- Rahina village at the core of the ancient capital Memphis, on the southern side of Saqqara to Bedrashein road, on a distance of 128 m south-west of Memphis open-air museum, and on a distance of 125 m south- east of the white walls chapel (Fig. 1). It was built of limestone by Ramesses II (the 19th Dynasty). The temple was originally found by the Egyptian army in 1969 while excavating for air raid shelters. Abdulla Sayed Mahmoud of the Ministry of Antiquities excavated the north part of the temple courtyard in 1970. Huleil Ghaly excavated the southern part of the temple in 1978, **(Mahmud, A.S, 1978)**. Further excavations took place in 1984, by Karim Abu Shanab, **(Excavations Reports, 1984)**. In 1985 the Egyptian exploration society planned the architectural elements of the temple (Fig. 2), **(Jeffreys, D.G, 1985)**. Hathor temple is partially excavated; orientated toward north/ south, and comprises a partially exposed colonnaded hall on the north. The columns of this hall have been decorated with inscriptions; their surmounted capitals have been carved from white limestone

in the shape of cubes (112x86x28cm), that they are likely to be Tura limestone, they are all very similar in the way that they have been carved, with Hathor as a woman's face and cow's ears carved in high relief on two opposite sides. The other two faces of the block are carved with locks of hair; there are slight differences in the carvings, especially in the way the smile is treated. The capitals are positioned so that Hathor faces looks outward and inward – so that on the northern row the faces look to the north and to the south, and on the western and eastern rows, the faces look out to the east and west. The southern and eastern sides of the temple are overlaid by later deposits and mud brick architecture. Stony remains of the temple are up to 5 meters below the present day surrounding ground surface, **(Mahmud, A.S, 1978)**.

The limestone remains of Hathor temple showed fine inscriptions, which are very fragile and highly endangered, where the temple suffered from serious damages after discovering, due to being exposed to climate changes, and it was left without any treatment until now. During the inspection of the Hathor temple, different kinds of alterations and degradation phenomena were evidenced, such as exfoliation, crumbling to splitting, cracking, gaps, open joints, discoloration, staining from bird droppings, missing parts, erosion of stone surfaces, disintegration, salt efflorescence, accumulates of dirt, pits, biological attacks by plants, graffiti and scratches (Fig. 3- 5).

A lot of deterioration factors and damage forces play an important role in degradation of limestone at Hathor temple. The most important deterioration factor affecting the temple is a salty ground water, which is considered the link between all other damage factors in the ancient Egyptian archaeological buildings, as they are considered the most important source of quick impact on construction materials including limestone. Moreover, it plays an important role in determining the effectiveness of some other ravages, **(Edgar, H, 2009., El Gohary, M, 2013, Mansour. A, 2019)**. Since we can't directly measure the level of the ground water around Hathor temple; so we use the level of surface water as indicator for the level of the ground water and for detection of variations in the levels. By follow-up it is turned out that the level of the ground water in Memphis varies around the year, as it is evident from the rise and fall of surface water ponds in the area. The main reasons for dramatic rising of water level at Mit- Rahineh are the increasing of irrigation and sewage water. Unfortunately, ground water had turned to become increasingly saline (rich in chlorides and different types of dissolved mineral salts) which is considered the most important physical weathering and destructive processes that affect physical and mechanical properties of the porous building materials, **(Goudie. A., Viles, H, 1997., Lavinia de Ferri, et al, 2011., Modestou, S, 2012)**. Where the salty ground water penetrates the lower parts of the engraved stone blocks and partly buried some parts and reached the exposed surfaces. The water, as it evaporates, leaves the salts in the pores, salts expand up to three times their volume as they form. This expansion acts like a wedge causing several damages such as cracks, breaking away small pieces of the stone, the surface layer peels off, detachment of the superficial layers and may cause for the large stone blocks to fall off, **(Carlos Rodriguez- Navarro, et al, 1999., Cardell. C, et al, 2003., Hosono, T, 2006., Jain, A, 2009)**. The wind and extensive changes in air temperature helps the crystallization/dissolution cycles of salts on the surface, which led to discoloration of stone surface, salt efflorescence, blistering, disintegration and formation of many salt encrustations on the reliefs, **(Ouacha, H, et al, 2013., Bala'awi. F, et al, 2019)**. The presence of high ground water has also encouraged the rapid growth of plants in the temple such as Polypogon monspeliensis (annual beard grass),

Phragmites australis (common reed), Schoenoplectus litoralis (khabb), Imperata cylindrica (halfa grass), and Alhagi graecorum (camel thorn). Growth of this plants are a threat for the stone blocks of Hathor temple, which are a source of attracting ground water under the foundations of the walls via its root system. Also when seeds grow in joints and small cracks of the stone, the root system expands the cracks eventually causing a calving off large pieces of stone, **(Mishra, A, K, et al, 1995., Lisci, M, 2003)** (Fig. 5d). Birds play a major role in the deterioration processes of limestone at Hathor temple, mechanically by some scratching and scraping forms. Chemically and biologically by creating some acidic central points through the deposition of guano, **(El Gohary, M, 2015)**. Air pollutants also contribute significantly to stimulate chemical weathering processes of metal components of saturated limestone with moisture in Hathor temple, which lead to erosion, as well as composition of the black crust on the stone surface, which largely leads to distortion of those surfaces, **(Anu Padma. R, et al, 2019., Venkat Rao. N, et al, 2014)**. In addition, the limestone blocks used in several of Hathor column capitals and numerous blocks in the west wall, it was carved and laid so the bedding planes of the mother rock are vertical rather than horizontal, which allows moisture to flow through the blocks freely and results in much more rapid deterioration (Fig. 4c, 4e, 5b). Also there are many human deterioration impacts, where it is believed that the former use of the temple as a quarry for building stones from the inhabitants of the village, as well as scratches graffiti on the stone surface (Fig. 4d).

The conservation of such types of structures exposed to environmental deterioration agents always represents a complex task, it is requiring a fundamental knowledge about the materials used in the construction process and understanding of the deterioration mechanism (**Cessari, et al. 2009**). Therefore, the conservation materials and techniques are used with the aim to preserve the current state of exposed carved limestone and also to achieve future preventive effect.

For the preservation and conservation of such structures and artworks, during the last 50 years, various synthetic polymers have been widely used; especially polymers based on acrylics, silicones, and mixture of them, moreover the lime water as a traditional consolidation material (**Daniele, et al. 2008**).

However, the conservation of outdoor limestone monuments using the polymers has created serious challenges, where some of them are characterized by the lack of compatibility with the original material of the object's substrate; moreover, they are subjected to degradation through the activities of weathering processes. Subsequently, it does not achieve the stability and efficiency for the long-term protection of outdoor monuments (**La Russaa et al. 2012**). Also the use of traditional material lime water results in an incomplete transformation of lime (calcium hydroxide) into calcium carbonate, leaving free particles on the surfaces and reducing the penetration of the material into the stone (**Arce and Indart 2015**). In the last decade, polymer nanocomposites have attracted great interest in the field of culture heritage conservation due to their unique properties (**Baglioni et al., 2012; Kapridaki and Maravelaki-Kalaitzaki., 2012**).

From the above, it has become clear that it is necessary that materials which are used in the consolidation and protection of limestone in Hathor temple must be compatible to its original material, able to improve its physical and mechanical properties, have the property of penetration and interaction inside the pores that are saturated with moisture, have the property

of hydrophobicity and be able to resist the deterioration factors, to achieve stability and efficiency for the long-term protection of outdoor monuments.

In the present study, four consolidants were used in the treatment of limestone samples which were collected from Memphis. The first one is (Acrisil 01/0. n), a ready for use product, a mixture of acrylic and silicone, while the second consolidante is (Estel 1100) a ready for use product, based on silicones, while the third one is nanocomposite that was prepared by adding nanoparticles of calcium hydroxide dispersed in ethyl-alcohol to the polymer of methyltrimethoxy silane, the fourth one is (Silres BS 290), a ready for use product, based on silicones.

This research aims to determine the efficiency of the used consolidants in order to select the best of them for the consolidation and protection of limestone in Hathor temple at Memphis. The properties of the treated limestone samples were comparatively investigated by visual appraisal, colorimetric measurements, static water contact angle, determination of physical properties of treated samples (bulk density, water absorption and apparent porosity), mechanical properties (Compressive strength, Abrasion resistance), and morphological characterization (the homogeneous distribution of consolidants on the stone surfaces) by scanning electron microscope. The stability and efficiency of the consolidants were evaluated by repeating the measurement of static water contact angle for the treated limestone samples after exposure to the artificial aging cycles.

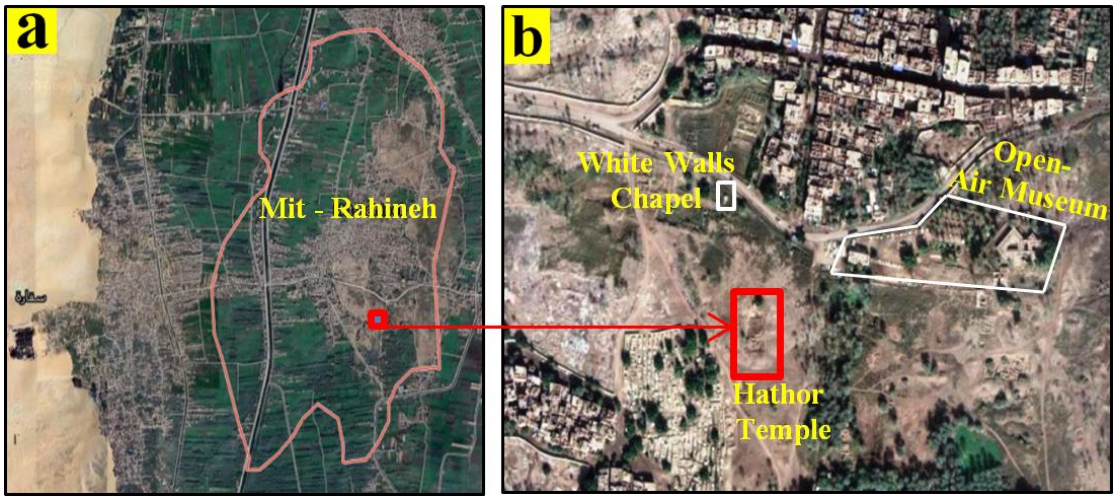

Fig.1. a) The site of Mit- Rahineh village (After: Google Earth), b) The site of Hathor temple in Mit-Rahineh village (After: Google Earth).

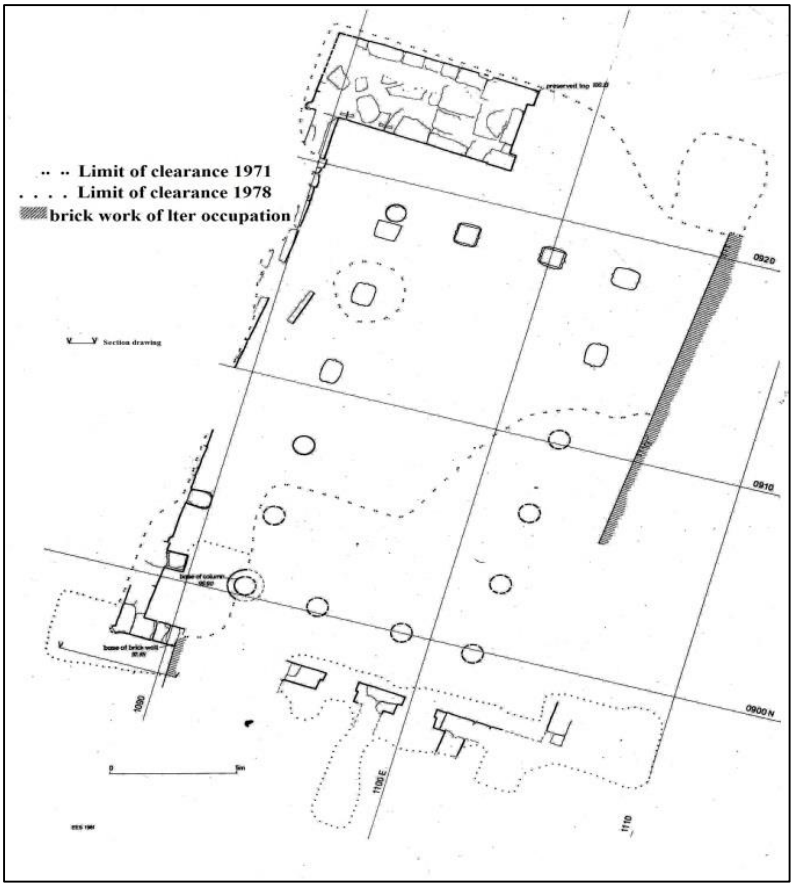

Fig.2) Plan of the Hathor Temple at Mit- Rahineh, Egypt. (After: Jeffreys, 1985).

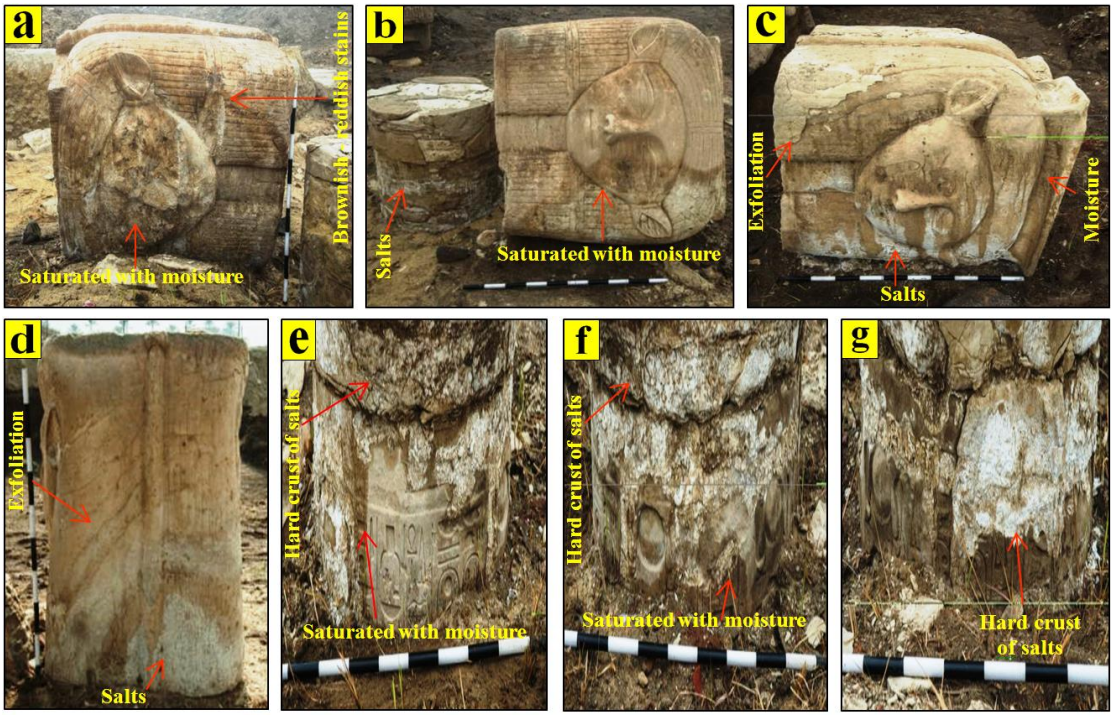

Fig.3a-g: Weathering forms of Hathor temple. a, b) downfall of Hathor column capital, being saturated with moisture, appearance of iron oxides as brownish stains. c, d) efflorescence of salts, exfoliation of stone surface as a result of sub efflorescence salts. e, f, g) saturated decorated columns with moisture and formation of hard crust of salts on the surface.

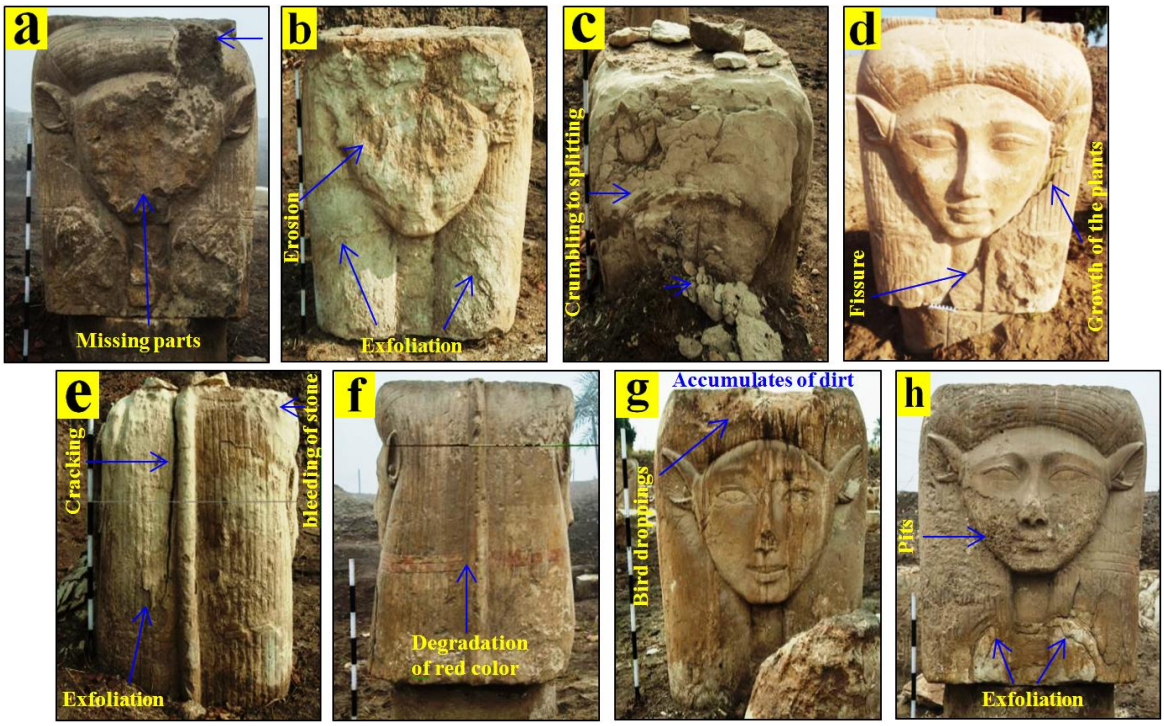

Fig.4a-h) Weathering forms of Hathor columns capitals at Hathor temple. a) missing parts of the column capital; b) exfoliation and erosion of stone surface; c) exfoliation of stone surface and crumbling to splitting; d) fissure and growth of the plants in the fissure; e) bleeding and degradation of the stone surface and large crack on the capital; f) degradation of the red color; g) accumulation of dirt and bird droppings; h) pits, and exfoliation of the stone surface.

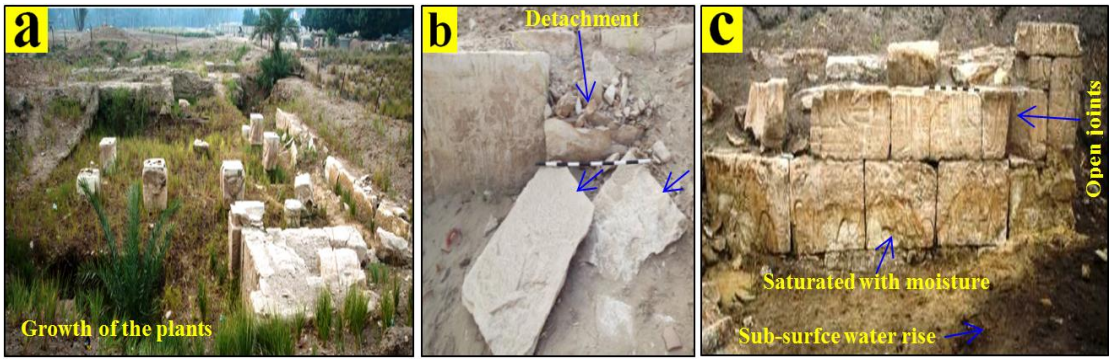

Fig.5a-c: Weathering forms of Hathor temple, a) growth of the plants in Hathor Temple, b) detachment of the superficial layer of wall, c) sub-surface water rise in the land of the temple, decorated thin limestone slabs saturated with moisture, open joints between the limestone slabs.

2. MATERIALS AND METHODS

2.1. Materials

2.1.1. Limestone samples

To characterize the limestone at Hathor temple, very small samples were collected from the fragments that have fallen from stone blocks, as a result of deterioration mechanisms. To apply the experimental study of the consolidants, some fragments of fallen limestone on the ground due to the distortion of some of the architecture elements which were exposed to ravages factors in the area, they were collected, and then were cut into cubic samples 3 cm^3.

2.1.2. Consolidation materials

In this study; four consoidants were used to consolidate of limestone samples which were collected from Memphis. The first consolidante is (Acrisil 201/0. n) (CTS, Italy), mixture of acrylic and silicone - organic solvent based product, combines good adhesion property of acrylic polymers and good penetration property of silicon polymers, (**Islam Saleh, et al, 2019**). The second consolidante is (Estel 1100) (CTS, Italy), mixture of ethyl silicate and poly siloxane - organic solvent based product. It was applied as a ready-to-use compound directly without dilution, suitable to consolidation of the stone-based monuments saturated with moisture, where it depends on moisture for polymerization interaction, **(Sayed Hemeda, et al, 2018)**. The third consolidante was prepared by mixing 50% of nanorestor (CTS, Italy) it is nanoparticles of calcium hydroxide $Ca(OH)_2$ 25g/liter dispersed in ethyl-alcohol, with 50% of MTMOS (Sigma-Aldrich, Germany) methyltrimethoxy silane based product, the selected percentage to compositions was suggested by several preliminary tests, which were carried out to produce a homogenous nanocomposite. The fourth consolidante is (SILRES BS 290) (Wacker Chemie, Germany), mixture of silane and siloxane - organic solvent based product, it has a good depth of penetration property, effective even on damp stones and have good water repellency, (**Dória Costa, et al, 2012., Jan Vojtěchovský, 2017., Ruba Ahmad, et al, 2018., Majid Hosseini, et al, 2018., Feigao Xu, et al, 2019**., **Alison Marie Rohly, 2019**).

2.2. Methods

2.2.1. Polarizing microscope

Nikon eclipse LV100POL polarizing microscope was used in the petrographic study of the collected limestone samples after being prepared as thin sections slides.

2.2.2. Scanning electron microscope

Quanta 250 scanning electron microscope (SEM), attached with EDX unit was used to investigate the limestone, crusts, and salts samples from Hathor temple. Moreover, it was used to examine and evaluate the ability of selected consolidants to preserve limestone samples in the experimental study. Also the attached EDX unit (Energy Dispersive X-ray Analysis) was used to perform the chemical analysis to the limestone, crusts, and salts samples from Hathor temple.

2.2.3. X ray diffraction analysis

XRD is considered the most famous method used in identification of crystalline compounds by their diffraction patterns. It plays an important role in the study of artworks, and also it helps in answering questions related to degradation processes, **(Garrison. E, 2003., Patnaik. P., Dean. S, 2004)**. The mineralogical composition for the collected samples was determined by means of x-ray diffraction analysis, which was performed using Philips analytical x-ray diffractometer. The operating conditions were gained through Cu k α radiation. The spectra were collected from 2-60 2θ; the scanning speed was 2θ = 1 degree/min. at constant voltage 40 kv, and 25 m A.

2.2.4. Physical properties

To determine the physical properties of the samples (bulk density, water absorption and apparent porosity) firstly; we must calculate the volume of each sample, weighting the dry and wet weight of each sample.

The physical properties were calculated as following, **(Sayed Hemeda, et al, 2018)**: -

- Bulk Density (D) in gm/cm^3 was determined as follows in equation:-

$$D = \frac{W}{V}$$

Where; (D) is the bulk density in gm/cm^3, (W) is the original weight in gm and (V) is the volume in cm^3.

- Water Absorption (W.A) in % was determined as follows in this equation: -

$$W.A = \frac{W_2 - W_1}{W_1} X\ 100 = \%$$

Where; (W. A) is the water absorption in %, (W1) dry weight of the sample in gm before immersion and (W2) saturation weight of the sample in gm after immersion in water for 24 h.

- Apparent porosity (A.P) in % was determined as follows in this equation: -

$$A.P = \frac{W_2 - W_1}{V} X\ 100 = \%$$

Where; (A.P) is the apparent porosity in %, (W1) the dry weight in gm, (W2) the wet weight in gm and (V) is the volume in cm^3.

2. 2. 5. Mechanical Properties

Hathor temple was subjected to mechanical deterioration factors. Therefore; the used consolidants must achieve improvement of mechanical properties of the construction materials. To determine the mechanical properties of the treated and untreated limestone samples, two types of mechanical tests mentioned below were conducted.

2.2.5.1. Compressive strength test

The measurement of compressive strength of the treated and untreated limestone samples were carried out using an Amsler compression-testing machine. According to ASTM C 170 (1976), the test was carried out on three limestone cubes (3 cm^3) for each consolidate, and the average values of compression strength were recorded.

2.2.5.2. Abrasion resistance test

Surface abrasion resistance of the treated and untreated samples was determined using Bohme abrasion wheel 1006, according to EN 14157 standard (2004) (Natural Stones —Determination of Abrasion Resistance). The abrasion system involved a 750-mm steel disk rotating at a speed of 30 cycles per minute with a solid steel counter weight applying a stress of 294±3 N. Twenty grams of abrasion dust (crystalline corundum Al_2O_3), was spread on the disk on which the sample was placed. This procedure was repeated 4 times by rotating each surface 90° in each step. After 16 cycles, the abrasion resistance was determined by calculating the percentage of the loss in weight for the limestone samples, **(Ibrahim Çobanolu, et al, 2010, Mehmedi Vehbi GÖKÇE, 2014)**.

2.2.6. Color alteration

Qualitatively, the nature of the color alteration can be understood by examining the visible reflectance spectrum before and after the samples have been treated using spectrophotometer. In this paper, the effects of consolidants on the general appearance of the treated limestone samples were determined by visual appraisal and the colorimetric measurements. The colorimetric measurements were carried out on the treated and untreated samples, in order to calculate and determine the variation of the general appearance properties induced by the treatments, using Optimatch 3100 spectrophotometer, based on the L*, a* and b* coordinates of the CIELAB color space, where L* is the lightness/darkness coordinate, a* the red/green coordinate (+a* indicating red and -a* green) and b* the yellow/blue coordinate (+b* indicating yellow and -b* blue), **(CIE Standard S014-4/E, 2007., Nabil. A, et al, 2016., Schanda, J, 2007, Darwish. S, 2013)**.

2.2.7. Hydrophobicity

The hydrophobicity of the treated samples were evaluated by measuring the static water contact angle using Drop master DM-701, fully automated contact angle meter.

2. 2. 8. Procedures of consolidation

The cubic limestone samples were washed by distilled water, and dried in an oven at 105 °C for at least 24 hours to reach constant weight, then it was left to cool at room temperature and controlled RH 50%, then it was weighed again (Licciulli, A, et al, 2011). To simulate the treatment as it happens in the archaeological field, the consolidation materials were applied onto the limestone samples by brushing until visible refusal. Treated samples were left for 1 month at room temperature and controlled RH 50% to allow the polymerization process to take place, **(Fatma M. Helmi, Yasser K. Hefni, 2016., Mohammad A. Aldosari, et al, 2019)**. The samples were weighted again, and the polymer uptake was calculated (Table 1).

2. 2. 9. The artificial aging

The stability and efficiency of consolidants for the long-term protection are very important requirements; especially for the stone-based archaeological features that are being exposed to natural weathering in outdoor environments. For this reason, simulating the climatic changes and the actual environmental deteriorating conditions which the temple is exposed to, from sunny to wet rainy weather conditions that were conducted, by the Wet- dry weathering cycles and ultraviolet. The treated samples were put in a temperature-controlled oven. This test consisted of 30 cycles alternatively between wet and dry as follows: 18 h of total immersion in distilled water then 2 h in room temperature and 4 h. at temperature controlled oven at 105 °C. Bearing in mind the exposure to a temperature of 60°C for a day is equivalent to 14 days in nature, and in the case of exposure to a temperature of 70°C for a day is equivalent to 27 days in nature, and in the case of exposure to a temperature of 100°C for a day is equivalent to 157 days in nature (**Blackshaw, S, et al, 1983**). Also the treated samples were irradiated with ultraviolet light working at 350 nm, 500 W for 45 days, (**Yang. L, et al. P, 2007**).

3. RESULTS AND DISCUSION

3.1. Characterization of Limestone at Hathor temple

The petrographic study revealed that the limestone samples of Hathor temple composed mainly of calcite as the major component associated with minor amount of dolomite and rare quartz, opaque minerals, iron oxides and halite. Calcite occurs as very fine- grained (micrite), anhedral crystals that represent the matrix of the sample. Dolomite occurs as very fine- grained anhedral crystals scattered in the matrix. Some irregular pore spaces are present in the carbonate matrix. Significant amounts of microfossils of different sizes and shapes are scattered in the matrix of the sample. Some microfossils are filled by recrystallized fine- grained carbonates. Some parts of the sample are stained by traces of irons. Opaque minerals are very fine to fine-grained and scattered in the sample as subhedral to anhedral crystals. (See Fig. 6).

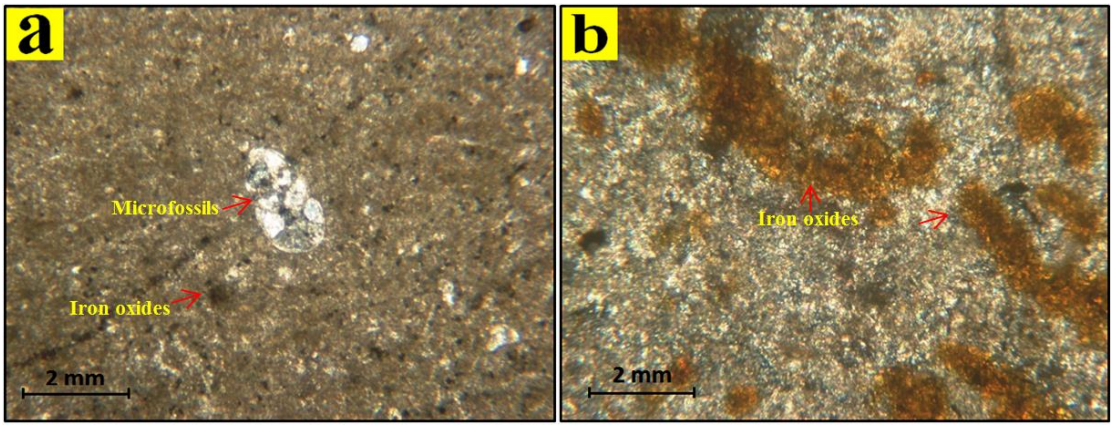

Fig. 6. a; b) Microphotographs of the stone samples under P.P.L.

The morphologic studies of limestone at Hathor temple by scanning electron microscope revealed the deterioration aspects, which are results of the aggressive weathering processes to which the temple have been subjected, such as granular disintegration, cavities, micro-exfoliation, dissolution of bonding materials and salt efflorescence, which leads to an increasing in porosity and loss of cohesion of the stone (Fig.7a, b). SEM micrograph indicated that most of limestone pores were affected by the salt crystallization and that crystals growing in small pores are able to exert sufficient pressure for the occurrence of granular disintegration, increased porosity and start or propagate cracks (Fig.7c). A dense coat of halite covers the stone surface, it was identified via its crystalline forms (cubic, prism and needles) (Fig.7d).

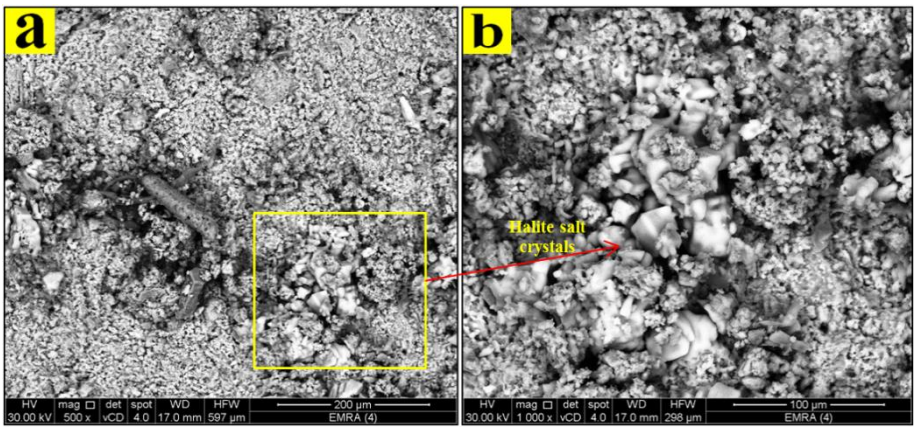

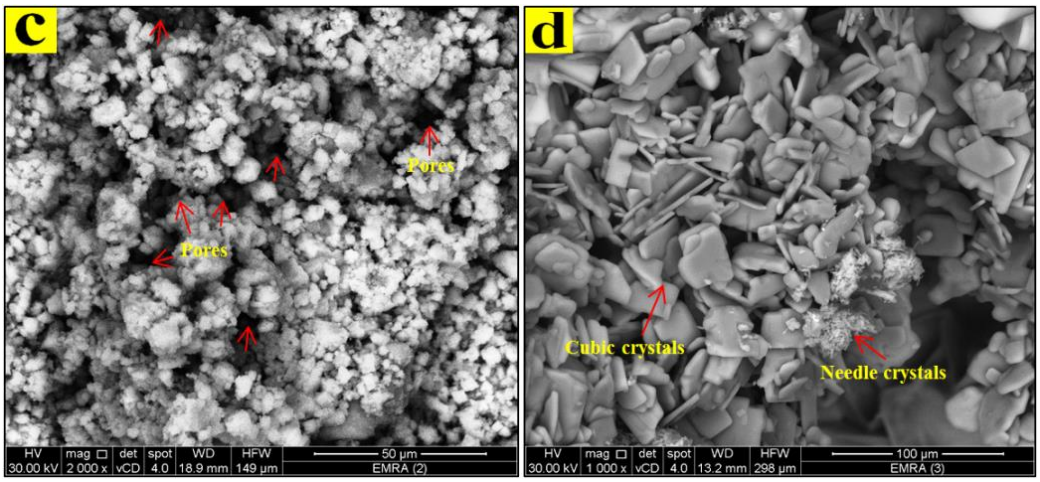

Fig. 7. SEM micrographs of limestone sample. a, b) Disintegration of stone surface and crystallization of halite as cubic aggregates in the pores; c) Disintegration of stone surface, d) a dense coat of halite crystals covers the stone surface.

The mineralogical and elemental characterization of the studied samples were carried out using x-ray diffraction analysis (XRD) and energy dispersive x-ray unit (EDX), respectively. XRD pattern of the limestone sample from Hathor temple (Fig. 8a) indicated that it mainly consists of calcite, in addition to dolomite and halite. The elemental analysis of the same sample (Fig. 8b) showed that it is composed of calcium, carbon, oxygen, chlorine, sodium, silicon, aluminum, magnesium, potassium and iron. Presence of peaks related to calcium (28.62 %), carbon (9.09 %) and oxygen (33.17 %) indicate the existence of calcium carbonate (calcite, $CaCO_3$) as a main component of limestone, which confirms the results of the petrographic study. The peaks of chlorine (8.02%) and sodium (7.91%) proved the presence of halite mineral. It is suggested that the salty ground water of Mit- Rahina is the main source of salts weathering, and presence of halite in the limestone composition at Hathor temple.

The mineralogical and elemental results of the archaeological limestone in Hathor temple, confirm the results of the petrographic and morphologic studies.

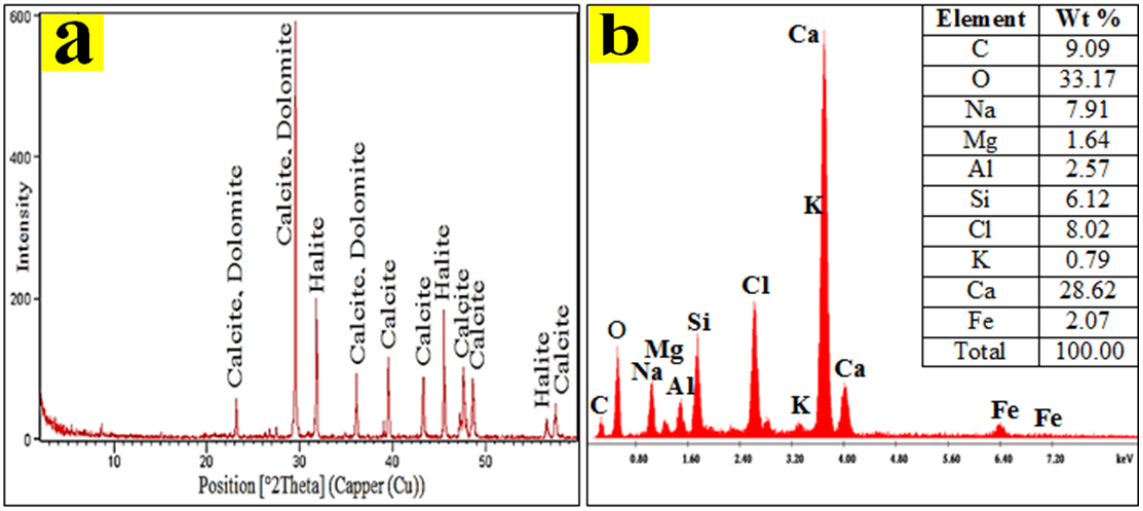

Element	Wt %
C	9.09
O	33.17
Na	7.91
Mg	1.64
Al	2.57
Si	6.12
Cl	8.02
K	0.79
Ca	28.62
Fe	2.07
Total	100.00

Fig. 8. a) XRD pattern of the limestone sample from Hathor temple; b) Elemental analysis pattern of the same sample.

4. Evaluation of consolidation materials

4.1. Physical properties of treated samples

All the used consolidation materials in this study, led to amelioration physical properties of the treated limestone samples, where all of them achieved increase of the bulk density, decrease of both apparent porosity and water absorption by varying degrees. The results of physical properties were reported in (Table 1).

By comparison, it is clear that the nanocomposite achieved the best results in improving the physical properties of the treated samples, as follows:

The treated samples by nanocomposite which is made up of (50% Nano restore + 50% M.T.M.O.S), achieved the highest bulk density of 2.72 gm/cm3 which is higher than the untreated sample by about 5.84% which was 2.57gm/cm3 (Fig. 9 a, d). Also this samples which was treated by nanocomposite achieved the lowest water absorption value of 1.09% which is lower than the untreated sample by about 83.18% which was 6.48% (Fig. 9 b, d). Also the lowest apparent porosity was achieved of 2.96% which is lower than the untreated sample by about 82.20% which was 16.63% (Fig. 9 c, d). So it can be suggested that the water absorption rates of the nanocomposites substantially depends on the chemical composition of the polymer used in their fabrication, (**Tsakalof, A, 2007**).

Table 1. The physical properties of the treated limestone samples.

Materials	Rate of increase in bulk density %	Rate of decrease in Water absorption %	Rate of decrease in apparent porosity %
Acrisil 01/0.n	2.33	76.08	75.53
Estel 1100	3.50	61.73	60.37
Nano restore + M.T.M.O.S	5.84	83.18	82.20
SILRES BS 290	4.28	63.27	61.69

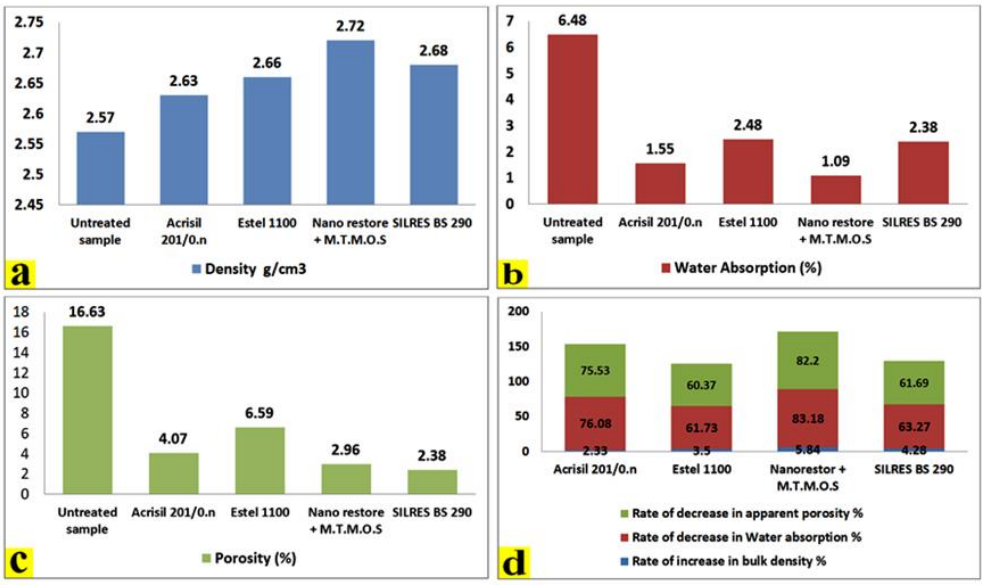

Fig. 9. The physical properties of the treated limestone samples. a) The average bulk density of treated and untreated limestone samples; b) The average water absorption of treated and untreated limestone samples; c) The average apparent porosity of treated and untreated limestone samples; d) Rates of amelioration in physical properties of treated limestone samples.

4.2. Mechanical Properties of treated samples

4.2.1. Compressive strength test

Measurement of compressive strength of treated and untreated limestone samples were achieved. The results were reported in (Table. 2, Fig. 10). Where the all consolidants were used in this study, led to amelioration of compressive strength to the limestone samples by varying degrees .

By comparison, we can observe the differences in compression strength values for treated and untreated limestone samples; it was observed that the samples treated with nanocomposite (Nano restore + M.T.M.O.S) gave the highest average values of compressive strength, amount to 16.2 MPa, by an increase of 90.59 % with respect to untreated samples, which give average values a compressive strength amount to 8.5 MPa. This can be attributed to ability of nanocomposite to penetrate easily into porous matrix of treated limestone samples, depending on the small size of calcium hydroxide nanoparticles, and low viscosity of methyltrimethoxy silane polymer. In addition to the effect of carbonation process of calcium hydroxide nanoparticles, high reactivity, fast reactions in the treated zones, and high compatibility with limestone samples. Moreover, hydrolyzed of methyltrimethoxy silane polymer by water to form silanols, which then polymerize in a condensation reaction and form a polymer that increases the cohesion of the stone material, (**Al-Omary. R, 2018, Mohammad A. Aldosari, 2017., Sierra-Fernandez. A, 2017**). While the treated samples by (Acrisil 01/0. n) achieved the second level in a compressive strength, amount to 14.9 MPa, by an increase of 75.29 % with respect to untreated sample. This can be attributed to the good adhesion properties of acrylic polymers which resulted in their relatively high surface free energy, which confirmed that the addition of acrylic polymers to silicon polymers has a positive effect in increasing their mechanical properties, (**Brus, J. and Kotlik, P, 1996**). While the treated limestone samples by (SILRES BS 290) and (Estel 1100) achieved the third and fourth levels respectively, in terms of average values compressive strength.

Table.2. The results of compressive strength to treated and untreated limestone samples.

Materials	Average value of compressive strength (MPa)	Rate of increase in compressive strength (%)
Untreated sample	8.5	0.00
Acrisil 01/0.n	14.9	75.29
Estel 1100	11.7	37.65
Nano restore + M.T.M.O.S	16.2	90.59
SILRES BS 290	12.6	48.24

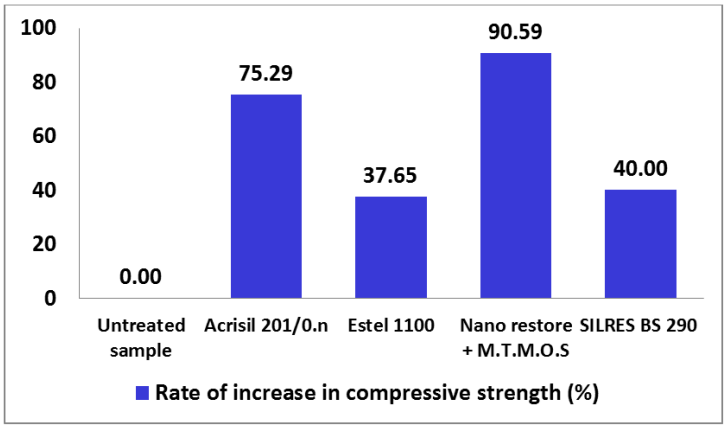

Fig. 10. The results of the compressive strength to the treated and untreated limestone samples.

4.2.2. Abrasion resistance

The abrasion resistance was determined using Bohme abrasion wheel 1006, by calculating the percentage of the loss in weight for the limestone samples. The results were reported in (Table. 3, Fig. 11). By comparison with untreated limestone sample. We can observe all used consolidants in this study led to amelioration of abrasion resistance to the limestone samples by varying degrees. It was observed that the treated samples by nanocomposite realized the best result in abrasion resistance. This may be as a result of nanoparticle properties and their role in enhancing the durability of the stone surface, improving also the interaction with the stone grains, **(Rob van Hees, et al, 2014)**.

Table.3. The results of the abrasion resistance test by Bohme abrasion wheel 1006.

Materials	Loss in weight (%)
Untreated sample	10.25
Acrisil 01/0.n	9.45
Estel 1100	9.65
Nano restore + M.T.M.O.S	9.11
SILRES BS 290	9.51

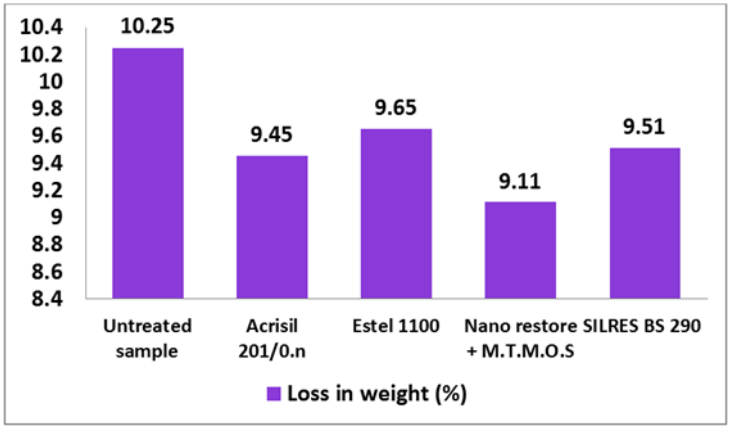

Fig. 11. Rates of the loss in weight of treated and untreated samples (%).

4. 3. Textural and morphological characterization after treatment

To evaluate the ability of the used consolidants in this study to consolidate and protect the limestone samples, comparative study of the textural and morphological characterization to the treated samples was performed by using scanning electron microscope. At the following, we can clarify the results of that study, as shown in (Fig. 12). Investigation by SEM of limestone sample treated by (Acrisil 201/0.n) showed non homogeneous distribution of the consolidant, and it was formed as thin film cussing close the pores of the stone surface (Fig.12a).

Investigation by SEM of treated limestone sample with (Estel 1100) showed the homogenous distribution of the consolidant and its ability to fill the small pores between the grains of the stone, inability to fill the wide pores, also it failed in covering and the binding between the large grains of the stone surface (Fig.12b)

Investigation by SEM of treated limestone sample with nanocomposite (50% Nano restore + 50% M.T.M.O.S), showed an excellent homogenous distribution for the consolidant on the stone surface, without closing the pore. Nanocomposite distributed in arranged way as network coating form, which allow to bind all grains on the stone surface. This indicates the strength of sample and its ability of water retardation (Fig. 12c).

Investigation by SEM of treated limestone sample with (SILRES BS 290) showed the homogenous distribution of the consolidant and its excellent ability to bind and cover the small grains and its acceptable ability to binding the large grains without covering them and without closing the pores of the stone surface (Fig. 12d). This indicates the efficiency of (SILRES BS 290) in the consolidation process, but not as the nanocomposite efficiency.

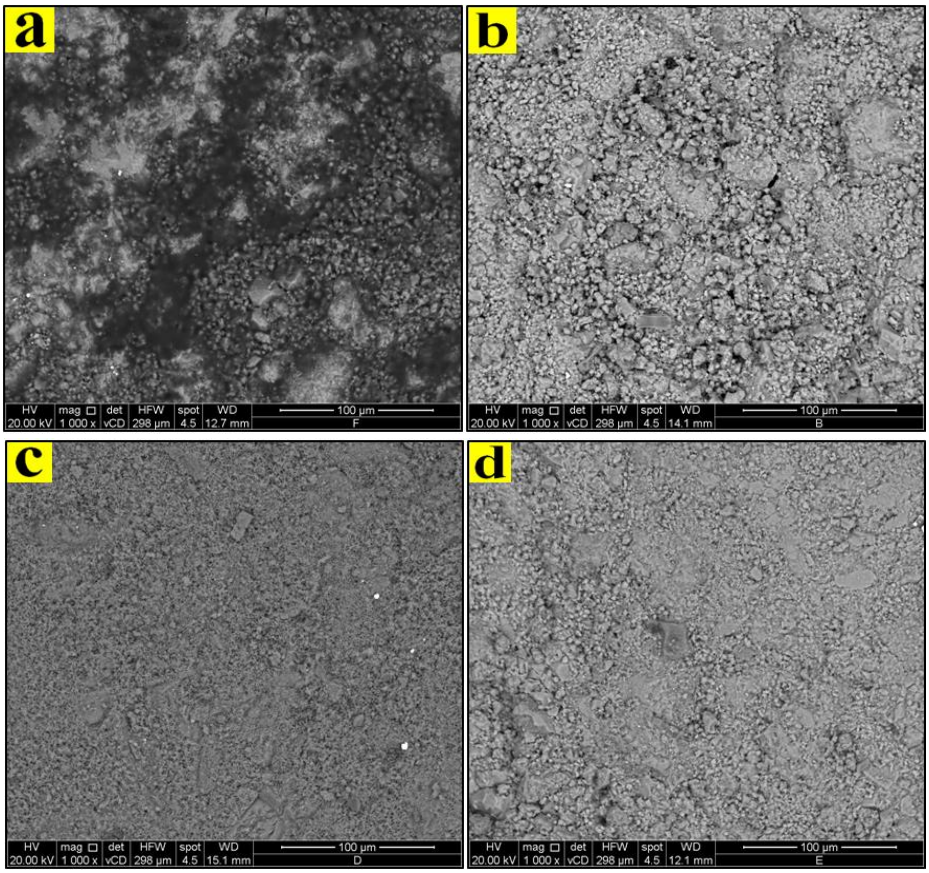

Fig.12. SEM micrographs to treated limestone samples with magnification 1000x. a), The treated sample with Acrisil 201/0. n; b), The treated sample with Estel 1100; c), The treated sample with nanocomposite; d) The treated sample with SILRES BS 290.

4.4. Static water contact angle

Some structural damage for the stone-based monuments around the world is caused by water and moisture from its various sources. But there is usually one simple remedy, preventive protection against moisture. So it is preferred that the used consolidants have property of water repellency, **(Lavinia de Ferri, 2011)**. To evaluate the water repellency of the treated samples, the static contact angle (sessile-drop method) of water droplets placed on different positions on the samples were measured, and the average values were taken. The untreated and treated samples were included in this test for comparison. Hydrophobicity of materials mainly depends on their chemical composition and structure. The Hydrophobicity scale of the surfaces is as follows, **(Parvate. S, et al, 2020).**

- Super hydrophilic material has water contact angle ($0° < \theta < 10°$).
- Hydrophilic material has water contact angle ($10° < \theta < 90°$).
- Hydrophobic material has water contact angle ($90° < \theta < 150°$).
- Super hydrophobic material has water contact angle ($150° < \theta < 180°$).

At the following, we can clarify the results of static water contact angle measurement, as shown in (Table. 4, Fig. 13,14). Where that all used consolidants in this study enhanced the property of water repellency of the limestone samples. Nanocomposite (50% nano restore + 50% M.T.M.O.S polymer) achieved highest degree of static water contact angle (152.4°). Hence it is classified as super hydrophobic material. This is attributed to hydrophobic character of (MTMOS) polymer, as a resulting in the presence of non-polar methyl group connected to the silicon atoms (the backbone in this polymer). Also to that the addition of Nano lime particles to the polymer of methyltrimethoxy silane resulted in super-hydrophobic nanocomposite, due to the surface roughness resulting from nanoparticles that lead to trapping of air between water droplets and the rough surface, which is illustrated in the Cassie-Baxter scenario, **(Cassie. B. D & Baxter. S, 1944., Michael, F. A, et al, 2009)**. While (SILRES BS 290) ranked second level in degree of the static water contact angle (126.2°), so it is considered a hydrophobic material. Acrisil 201/0. n had achieved an unsatisfactory result of the static water contact angle value (67.9°), so it is considered as a hydrophilic material. But (Estel 1100) achieved the lowest static water contact angle value, where it loses the organic radical (Ethyl groups) when it reacts with water (Hydrolysis process).

Table.4. Results of Static water contact angle test of the treated and untreated limestone samples.

Materials	Static Contact angle (º)
Untreated sample	25.8 º
Acrisil 201/0.n	67.9 º
Estel 1100	46.9 º
Nano restore + M.T.M.O.S	152.4 º
SILRES BS 290	126.2 º

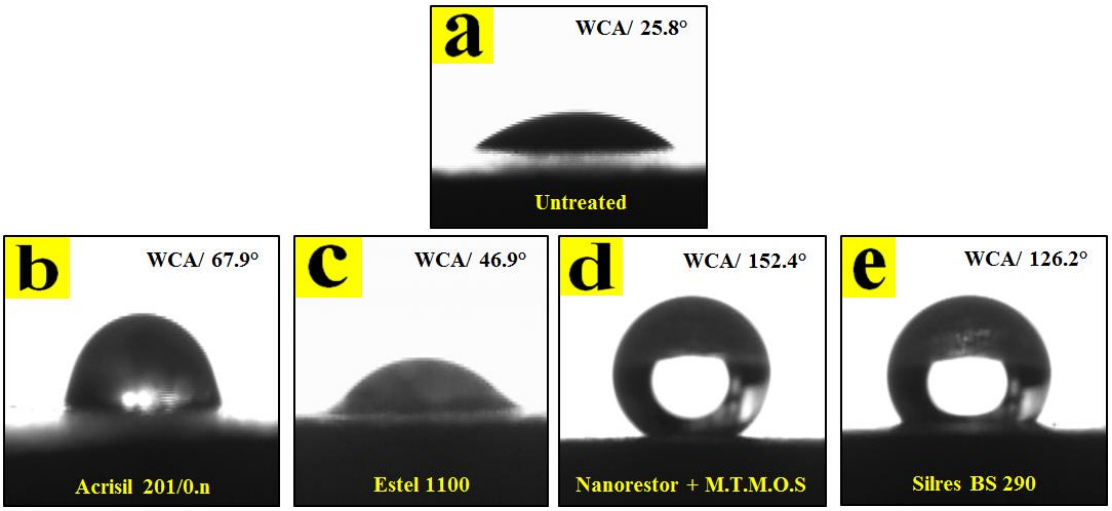

Fig.13. Photographs of water droplets on the treated and untreated limestone samples.

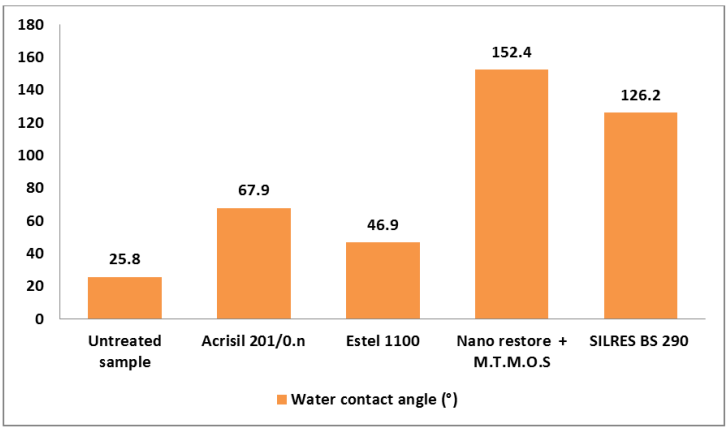

Fig. 14. Rates of static water contact angle to the treated and untreated limestone samples.

4.5. Aesthetical properties

To evaluate the aesthetic alteration of the treated limestone samples, visual appraisal and colorimetric measurements were carried out. The visual appraisal to the samples is depending on the color difference between the treated and untreated limestone samples. (Fig.15) general appearance of the treated and untreated samples.

By the visual appraisal, it was found that (Acrisil 201/0.n) led to a significant darkness in the color of treated samples. While (Estel 1100) led to a slight yellowness of the treated samples. While nanocomposite (50% nanolim + 50% M.T.M.O.S) didn't have a noticeable effect on the color of the samples. But the (SILRES BS 290) led to very slight change in the color of the treated samples.

Fig .15. General appearance of the treated and untreated samples.

The chromatic changes ΔE^*_{ab} were carried out by means of Optimatch 3100 spectrophotometer, in order to calculate and determine the variation of the aesthetical properties induced by the treatments, according to the following equation:-

$$\Delta E^*_{ab} = \sqrt{[(\Delta L^*)^2 + (\Delta a^*)^2 + (\Delta b^*)^2]}$$

Where ΔL*, Δa* and Δb* are the differences in the, L*, a* and b* coordinates (according to CIELAB color space) of the treated and untreated limestone samples.

The ΔE scale in stone materials conservation is as follows, **(Limbo. S, et al, 2006)**:-

- $\Delta E < 0.2$: not perceptible difference.
- $0.2 < \Delta E < 0.5$: very small difference.
- $0.2 < \Delta E < 0.5$: small difference.
- $2 < \Delta E < 3$: fairly perceptible difference.
- $3 < \Delta E < 6$: perceptible difference.
- $6 < \Delta E < 12$: strong difference.
- $\Delta E > 12$: different colors.

As according to guidelines for conservation purposes of historical or monumental surfaces, the ΔE value must be < 5, **(Giovanni. B. G, et al, 2015., NorMal, R, 2017., Francesca. P, et al, 2018)**.

The ΔE*ab values obtained from the chromatic measurements of the treated and untreated limestone samples (Table. 5, Fig.16), confirmed the results of the visual appraisal. Where that the treated samples with nanocomposite (50% nanolim + 50% M.T.M.O.S) achieved lowest value of total color change ΔE*ab amount to (2.25), which below the threshold values according to guidelines for conservation purposes. Also the treated samples with (SILRES BS 290) achieved value of total color change ΔE*ab amount to (3.16), which also did not exceed guidelines values of conservation purposes. But the treated samples by (Estel 1100) achieved value of ΔE*ab amount to (5.18). While the treated samples by (Acrisil 201/0. n) achieved largest value of total color change ΔE*ab amount to (9.47), exceeding guidelines values of conservation purposes, so it failed to conserve the natural color of the treated samples.

Table.5. Results of the chromatic measurements of the treated samples.

Materials	**ΔL^***	**Δa^***	**Δb^***	**ΔE^***
Acrisil 201/0.n	8.66	0.35	3.82	9.47
Estel 1100	1.22	-0.36	-5.02	5.18
Nano restore + M.T.M.O.S	-1.94	-0.20	1.12	2.25
SILRES BS 290	-0.08	0.00	3.13	3.13

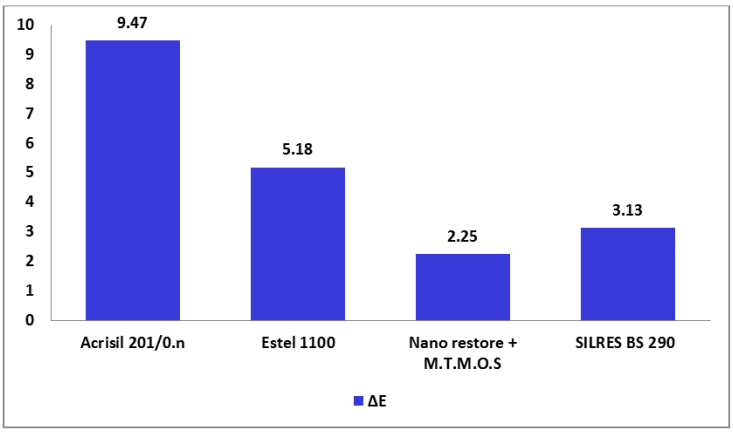

Fig .16. Results of the chromatic measurements of the treated samples.

4.6. The stability and efficiency of consolidants

The stability and efficiency of the consolidants are very important requirements; especially for the stone-based archaeological features that are being exposed to natural weathering in outdoor environments.

To evaluate the effects of the exogenous deterioration factors on the treated limestone samples, the static water contact angle measurement was repeated after exposing to the artificial aging procedures.

For all consolidants, the values of static water contact angle clearly were reduced after exposure to the artificial aging, as shown in (Table. 6, Fig.17, 18). This can be attributed to effects of the Wet-dry weathering cycles and the photo-oxidative effect of ultraviolet, which is considered to be one of the most deterioration factors of polymers. It was also observed that the nanocomposite is more resistance to artificial aging compared to other used consolidants. This can be attributed to the carbonation process of calcium hydroxide nanoparticles Ca $(OH)_2$, high reactivity, fast reactions in the treated zones, high compatibility with limestone, and high stability at different conditions, **(Chelazzi. D, et al, 2012., Baglioni. P, et al, 2008)**. This can also be attributed to the role of calcium hydroxide nanoparticles particles in improving the physical and mechanical properties of M.T.M.O.S polymer.

Table.6. Static water contact angle of treated limestone samples after exposure to artificial aging.

Materials	Static Contact angle (º)
Acrisil 201/0.n	45.6 º
Estel 1100	32.9 º
Nano restore + M.T.M.O.S	140.5 º
SILRES BS 290	112.6 º

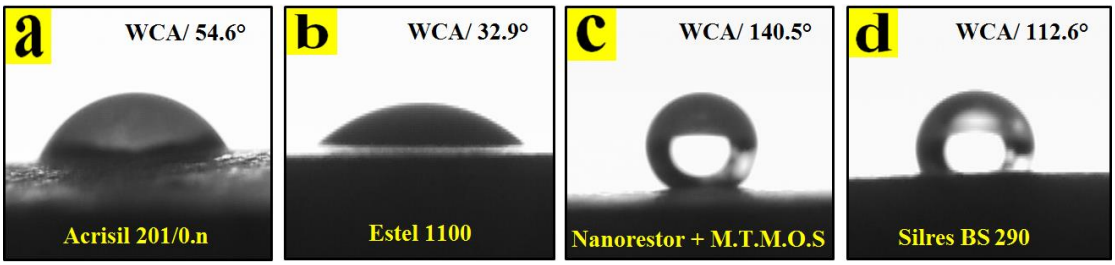

Fig.17. Photographs of water droplets on the treated limestone samples after exposure to artificial aging.

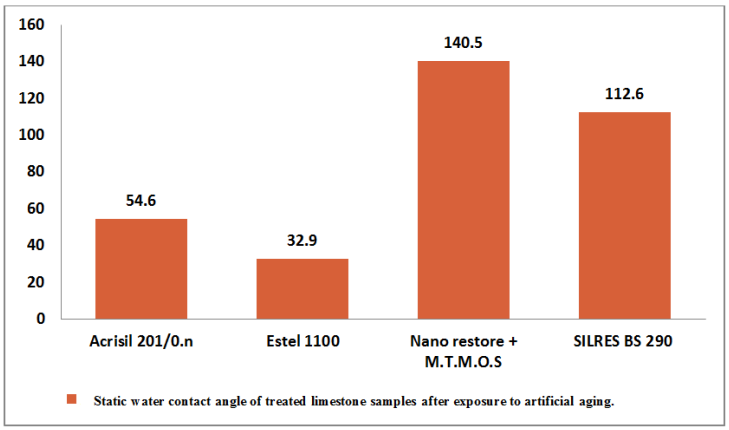

Fig .18. Rates of static water contact angle to the treated limestone samples after exposure to artificial aging.

5. CONCLUSIONS

The main important damage factors of Hathor temple at Mit- Rahina village are the salty ground water, rains, variation of temperature, salts, air pollutions, human and biological factors.

different kinds of alterations and degradation phenomena to the limestone in Hathor temple were evidenced, such as exfoliation, crumbling to splitting, cracking, gaps, open joints, discoloration, staining from bird droppings, missing parts, erosion of stone surfaces, disintegration, salt efflorescence, accumulates of dirt, pits, biological attacks by plants, graffiti and scratches.

Investigation and analytical methods showed that archeological limestone in Hathor temple consist mainly of very fine grains of calcite, with minor amount of dolomite and rare quartz, opaque minerals, iron oxides and halite, with microfossils of different sizes and shapes. It also suffers different kinds of alterations and degradation phenomena.

In this study, the efficiency of four consolidates (Acrisil 01/0. n, Estel 1100, Nano restore + M.T.M.O.S, Silres BS 290) to determine comparatively what are the best of them to be used it in the consolidation and protection of the limestone at Hathor temple, and which can prevent any future damage. The results showed that the nanocomposite (Nano restore + M.T.M.O.S) is the most suitable material for consolidation and protection of the limestone samples, where it achieved an excellent distribution and formed a homogeneous coating on the stone surface without closing the pores, as observed by SEM microscopic investigation.

The nanocomposite (Nano restore + M.T.M.O.S), achieved the best values of amelioration in the physical properties of limestone samples as follows:

- Rate of increase in bulk density to the treated limestone samples (5.84%).

- Rate of decrease in Water absorption to the treated limestone samples (83.18%).
- Rate of decrease in apparent porosity o the treated limestone samples (82.20%).

The nanocomposite (Nano restore + M.T.M.O.S) achieved the best values of amelioration of the mechanical properties of limestone samples as follows:

- Rate of increase in compressive strength to the treated limestone samples (90.59%).
- Abrasion resistance test - Loss in weight to the treated limestone samples (9.11%).

The nanocomposite (Nano restore + M.T.M.O.S) achieved highest degree of static water contact angle to the treated samples (152.4°), so it is considered an ultra-hydrophobic material.

The nanocomposite (Nano restore + M.T.M.O.S) achieved the best results in terms of preserving the aesthetical properties of treated limestone samples, where it achieved lowest value of total color change ΔE*ab to the treated limestone samples amount of (2.25), which below the threshold values according to guidelines for conservation purposes, as observed by colorimetric test.

The nanocomposite (Nano restore + M.T.M.O.S) showed the high compatibility with limestone samples. It also showed the best result from where the resistance of artificial aging procedures. So it was able to achieve the stability and efficiency for the long-term protection of outdoor monuments and to achieve the future preventive effect.

We think that the obtained results will help in providing an image concerning current conservation state of Hathor temple, as well as establishing a conservation plan of this temple.

6. RECOMMENDATIONS

It is recommended to apply the following points:

- Completion of the excavation work of the Hathor temple at Mit- Rahina.
- Removing the crystallized salts on the surfaces of the architectural elements in the Hathor temple at Mit- Rahina .
- Biological control of plant growth in the Hathor temple at Mit- Rahina, by mechanical and chemical methods.
- Implementation of the project to reduce the level of ground water in the archaeological area, which the Hathor temple is located.
- Using nanocomposite which consists of (50% Nano restore + 50% M.T.M.O.S) to consolidate and protect the limestone in Hathor temple at Mit- Rahina.

7. References

1. Alison Marie Rohly. (2019) Improving Sustainability in Protective Coating Systems, A Dissertation Submitted to the Graduate Faculty of the North Dakota State, University of Agriculture and Applied Science, In Partial Fulfillment of the Requirements for the Degree of Doctor of Philosophy.

2. Anu Padma. R, Ramasamy. R, Mathews. M.S. (2013) Chemical Weathering of A Granite Stone Sample from The Peruvudaiyaar Koil, Thanjavur, Tamil Nadu, India, IOSR Journal of Applied Geology and Geophysics (IOSR-JAGG), Vol.1, Issue (2), pp. 39-53.

3. Arce LP, Indart ZA. (2015) Carbonation Acceleration of Calcium Hydroxide Nanoparticles: Induced by Yeast Fermentation. Applied Physics A, Vol. 120, Issue (4), pp.1475-1495.

4. ASTM C. American Society for Testing. (1976) and Protection of Stone Monuments. Standard Test Methods for Compressive Strength of Natural building stone, ASTM C 170; UNESCO: Paris.
5. Baglioni, P., Giorgi, R., Chelazzi, D. (2012) Nano-materials for the Conservation and Preservation of Movable and Immovable Artworks, Progress in Cultural Heritage Preservation, pp. 313-318.
6. Baglioni. P, Giorgi. R, Dei. L. (2008) Soft Condensed Matter for the Conservation of Cultural Heritage, Materials Forum, Vol. 32, pp. 121- 128.
7. Bala'awi. F, Alshawabkeh. Y, Al masri. E, Mustafa. M.H. (2018) Salt Damage and Environmental: A thermodynamic Approach from The Northern Roman Theater in Jerash, JORDAN, Journal of Mediterranean Archaeology and Archaeometry, Vol. 18, No 2, pp. 49-66.
8. Black Shaw, S. M & Ward, S. E. (1983) Simple Tests for Assessing Materials for use in Conservation, Department of Scientific Research and Conservation, British Museum, London, pp. 1-15.
9. Brus, J. and Kotlik, P. (1996) Consolidation of Stone by Mixtures of Alkoxysilane and Acrylic Polymer, Studies in Conservation, Vol. 41, No. 2, pp. 109 : 119.
10. Cardell. C, Delalieux. F, Roumpopoulosb. K, Moropouloub. A, Augerc. F, Van Griekena. R. (2003) Salt-Induced Decay in Calcareous Stone Monuments and Buildings in A marine Environment in SW France, Journal of Construction and Building Materials, Vol. 17, pp. 165–179.
11. Carlos Rodriguez- Navarro& Eric Doehne. (1999) Salt Weathering: Influence of Evaporation Rate, Super saturation and Crystallization Pattern, Earth Surface Processes and Landforms, Vol. 24, pp. 191- 209.
12. Cassie. B. D & Baxter. S. (1944) Wettability of Porous Surfaces, Trans. Faraday Soc., no. 5, pp. 546–551.
13. Cessari L, Cenzia B, Elena G, Maria G. (2009) sustainable technologies for diagnostic analysis and restoration techniques: the challenges of the green conservation. Proceedings of the 4th international congress science and Technology for the Safeguard of cultural heritage of the Mediterranean Basin, Cairo, Egypt.
14. Chelazzi. D, Poggi. G, Jaidar. Y, Toccafondi. N, Giorgi. R, Baglioni. P. (2012) Hydroxide Nanoparticles for Cultural Heritage, Consolidation and Protection of Wall Painting and Carbonate Material, Journal of Colloid and Interface Science, pp. 1- 18.
15. CIE Standard S014-4/E. (2007) Colorimetrys, part 4: CIE 1976 L*a*b* colour space.
16. Daniele V, Taglieri G, Quaresima R (2008) The nanolimes in Cultural Heritage Conservation: Characterization and Analysis of the Carbonatation Process. Journal of Cultural Heritage, Vol. 3, Issue (9), pp. 294–301.
17. Darwish. S. S. (2013) Evaluation of The Effectiveness of Some Consolidants Used for The Treatment of The XIXTH Century Egyptian Cemetery Wall Painting, International Journal of Conservation Science, Vol. 4, Issue (4), pp. 413-422.
18. Dória Costa, José Delgado Rodrigues. (2012) Consolidation of a Porous Limestone with Nanolime, 12th International Congress on the Deterioration and Conservation of Stone.
19. Edgar, H. C. (2009) A ground Water Flow Model for Water Related Damages on Historic Monuments, Case Study West Luxor, Egypt, Department of Water Resources Engineering Faculty of Engineering, Lund University, Sweden.

20. EL-Gohary. M. (2015) Effective Roles of Some Deterioration Agents Affecting Edfu Royal Birth House "Mammisi", International Journal of Conservation Science, Vol. 6, Issue (3), pp. 349-368.
21. EL-Gohary. M. (2013) Physical Deterioration of Egyptian Limestone Affected by Saline Water, International Journal of Conservation Science, Vol. 4, Issue (4), pp. 447-458.
22. Excavations Reports of The supreme Council of Antiquities, Mit Rahina, Seasons 1978& 1984.
23. Fatma M. Helmi1, Yasser K. Hefni. (2016) Nanocomposites for The Protection of Granitic Obelisks at Tanis, Egypt, Mediterranean Archaeology and Archaeometry, Vol. 16, No 2, pp. 87-96.
24. Feigao Xu, Weiping Zeng, Dan Li. (2019) Recent advance in Alkoxysilane-based Consolidants for Stone, Progress in Organic Coatings 127, pp. 45- 54.
25. Francesca. P., Antonella. P., Alessandra. T., Mariateresa. L., Maurizio. M., Angela. C., Lucia. M. C, Roberto. C., (2018) TiO_2 Nanocrystal Based Coatings for the Protection of Architectural Stone: The Effect of Solvents in the Spray-Coating Application for a Self-Cleaning Surface, Coatings, 8, 356, pp. 1- 23.
26. Garrison. E. G. (2003) Techniques in Archaeological Geology, Springer, German, p. 212.
27. Giovanni. B. G & Placido. M. (2015) Preservation of Historical Stone Surfaces by TiO2 Nano coatings, Coatings, 5, pp. 222-231.
28. Goudie. A., Viles, H. (1997) Salt Weathering Hazards, John Wiley & Sons, p.241.
29. Hosono, T., Uchida, E., Suda, C., Ueno, A., Nakagawa, T. (2006) Salt Weathering of Sandstone at the Angkor Monuments, Cambodia: Identification of the Origins of Salts Using Sulfur and Strontium Isotopes, Journal of Archaeological Science, Vol. 33, pp. 1541–1551.
30. Ibrahim Çobanolu, Sefer Beran Çelik and Devrim Alkaya. (2010) Correlation between "Wide Wheel Abrasion (Capon)" and "Bohme Abrasion" Test Results for Some Carbonate Rocks, Scientific Research and Essays Vol. 5, (22), pp. 3398-3404.
31. Islam Saleh1, Mohamed Abdel Hady, Abubakr Moussa, Yasser Hefni, M.L. Abd El-latif. (2019) Experimental Study for the Consolidation and Protection of Sandstone Petroglyphs at Sarabit El Khadem (Sinai, Egypt), Scientific Culture, Vol. 5, No. 1, pp. 43-48.
32. Jain, A., Bhadauria, S., Kumar, V., Chauhan, R. (2009) Bio deterioration of Sandstone Under The influence of Different Humidity Levels in Laboratory Conditions, Building and Environment, Vol. 44, pp. 1276-1248.
33. Jan Vojtěchovský. (2017) Surface Consolidation of Wall Pantings Using Limenano-Suspensions, Acta Polytechnica 57, (2), pp. 139–148.
34. Jeffreys, D.G. (1985) The Survey of Memphis I, The Archaeological Report, Occasional Publications 3, London, p. 38.
35. Kapridaki, C. and Maravelaki- Kalaitzaki, P. (2012) TiO_2-SiO_2-PDMS Nano-composite Hydrophobic Coatings with Self-cleaning Properties for Marble Protection, Progress in Organic Coatings, 76, pp. 400-410.
36. La Russaa FM, Ruffolo AS, Rovellaa N et al (2012) Multifunctional TiO2 coatings for cultural heritage. Prog Org Coat 74:186–191.

37. Lavinia de Ferri, Pier Paolo Lottici, Andrea Lorenzi, Angelo Monteneroc, Emma Salvioli-Mariani. (2011) Study of Silica Nanoparticles – Polysiloxane Hydrophobic Treatments for Stone-Based Monument Protection, Journal of Cultural Heritage 12, pp. 356–363.

38. Licciulli, A., Calia, A., Lettieri, M., Diso, D., Masieri, M., Franza, S., Amadelli, R., Casarano, G. (2011) Photocatalytic TiO_2 Coatings on Limestone. Journal of Sol-Gel Science and Technology, 60, pp. 437–444.

39. Limbo. S, Piergiovanni. L. (2006) Shelf Life of Minimally Processed Potatoes Part 1 Effects of High Oxygen Partial Pressures in Combination with Ascorbic and Citric Acids on Enzymatic Browning, Postharvest Biology Technology, 39, pp. 254–264.

40. Lisci, M., Monte, M., Pacini, E. (2003) Lichens and Higher Plants on Stone: A review, International Biodeterioration& Biodegradation, Vol. 51, pp. 1-17.

41. Mahmud, A.S. (1978) A New Temple for Hathor at Memphis, Warminster, Aris & Phillips Ltd, England.

42. Majid Hosseini, Ioannis Karapanagiotis. (2018) Advanced Materials for the Conservation of Stone, Springer International Publishing AG.

43. Mansour. A., El Attar. R.M. (2019) Assessment of Salt Damage Based on Crystallization Test Due to High Groundwater Level in Sandstone Monuments, Luxor, Egypt, International Journal of Scientific & Engineering Research Volume 10, Issue (11), pp. 1352-1360.

44. Mehmedi Vehbi GÖKÇE. (2014) The effects of Bedding Directions on Abrasion Resistance in Travertine Rocks, Turkish Journal of Earth Sciences 24, pp. 196-207.

45. Michael, F. A., Paulo, J. F., Daniel, L. S.(2009) Nanomaterials: Nanotechnology and Design An Introduction for Engineers and Architects, Nanotechnology and Nanomaterials an Overview, Chaptr 1, Elsevies Ltd, pp. 1-16.

46. Mishra, A, K., Jian, K. K., Garg, K. L. (995) Role of Higher Plants in The Deterioration of Historic Buildings, Journal of The Science of the Total Environment, vol. 167, pp. 375- 392.

47. Modestou, S., Theodoridou, M., Loannou, L., Fournari, R. (2012) Micro-Destructive Mapping of Salt Crystallization in Stone" 12th International Congress on The Deterioration and Conservation of Stone, pp. 20.

48. Mohammad A. Aldosari & Sawsan S. Darwish & Mahmoud A. Adam& Nagib A. Elmarzugi& Sayed M. Ahmed. (2019) Evaluation of Preventive Performance of Kaolin and Calcium Hydroxide Nanocomposites in Strengthening the Outdoor Carved Limestone, Archaeological and Anthropological Sciences, 11, pp.3389–3405.

49. Mohammad A. Aldosari & Sawsan S. Darwish & Mahmoud A. Adam& Nagib A. Elmarzugi & Sayed M. Ahmed. (2017) Protecting of Marble Stone Facades of Historic Buildings Using Multifunctional TiO_2 Nano coatings, Sustainability 9(2002), pp. 2–15.

50. Nabil A. Abd EL-Tawab Baderi, Ala M. Ashry. (2016) The Cleaning of The Isis Temple's Mural Paintings in Upper Egypt Using Zinc Oxide Nanoparticles and Non-ionic Detergent, International Journal of Conservation Science, Vol. 7, Issue (2), pp. 443-458.

51. NorMal, R. Misure Colorimetric The Strumentali di Superfici Opache. Availableonline:http://www.architettiroma.it/fpdb/conultabc/File/ConsultaBC/Lessic _NorMal-Santopuoli.pdf (accessed on 2 August 2017).

52. Ouacha, H., Ben Moussa, A., Simao, J. (2013) The Salt Crystallization Weathering of Building Rocks of the Archaeological Sites Calcarenites of North-Western Morocco (Lixus, Banasa and Thamusida). European Scientific Journal vol.9, No.18, pp. 282- 290.
53. Patnaik. P., Dean. S. (2004) Analytical Chemistry Handbook, McGraw-Hill, Second Edition, p.922.
54. Rob van Hees, Lubelli B, Nijland T, Bernardi A. (2014) Compatibility and Performance Criteria for Nanolime Consolidants, in: Proceedings of the 9th International Symposium on the Conservation of Monuments in the Mediterranean Basin - Monubasin, Ankara.
55. Ruba Ahmad Al-Omary., Mustafa Al-Naddaf., Wassef Al Sekhaneh. (2018) Laboratory Evaluation of Nanolime Consolidation of Limestone Structures in The Roman Site of Jerash, Jordan, Mediterranean Archaeology and Archaeometry, Vol. 18, No 3, pp. 35-43.
56. Sayed Hemeda, Mervat Khalil, Ahmed Shoeb, Ahmed Abd EL Aziz. (2018) The effectiveness of Nano Materials and Nano- Modified Polymers for Preservation of Historic Brick Masonry in Rashid, Egypt, International Journal of Conservation Science Vol. 9, Issue (4), pp.835-846.
57. Schanda, J. (2007) Calorimetry, Wiley-Inter-science, John Wiley & Sons Inc, p. 56.
58. Sierra-Fernandez. A, Gomez-Villalba. L.S, Rabanal. M.E., Fort. R. (2017) New Nanomaterials for Applications in Conservation and Restoration of Stony Materials: A review, Materiales de Construcción, Vol. 67, Issue (325), pp. 1- 18.
59. Sumit Parvate, Prakhar Dixit, and Sujay Chattopadhyay. (2020) Superhydrophobic Surfaces: Insights from Theory and Experiment, the Journal of Physical Chemistry B, 124, (8), pp. 1323-1360.
60. Tsakalof, A., Manoudis, P., Karapanagiotis, I., Chryssoulakis, I., Panayiotou, C. (2007) Assessment of Synthetic Polymeric Coatings for The Protection and Preservation of Stone Monuments, Journal of Cultural Heritage, Vol. 8, pp. 69-72.
61. Venkat Rao. N, Rajasekhar. M, Chinna Rao. G. (2014) Detrimental Effect of Air Pollution, Corrosion on Building Materials and Historical Structures, American Journal of Engineering Research (AJER), Vol.3, Issue (03), pp-359-364.
62. Yang. L, Wang. P. (2007) Investigation of Photo-stability of Acrylic Polymer Paraloid B72 Used for Conservation, Sciences of Conservation and Archaeology 19, pp. 54–58.